

Unveiling Triangular Correlation of Angular Deviation in Muon Scattering Tomography by Means of GEANT4 Simulations

A. Ilker Topuz,^{1,2} Madis Kiisk,^{1,3} Andrea Giammanco,² and Mart Magi³

¹*Institute of Physics, University of Tartu, W. Ostwaldi 1, 50411 Tartu, Estonia*

²*Centre for Cosmology, Particle Physics and Phenomenology, Université catholique de Louvain, Chemin du Cyclotron 2, B-1348 Louvain-la-Neuve, Belgium*

³*GScan OU, Maealuse 2/1, 12618 Tallinn, Estonia*

Corresponding author: A. Ilker Topuz

Email: ahmet.ilker.topuz@ut.ee

Abstract

The angular deviation commonly represented by the scattering angle generally serves to provide the characteristic discrimination in the muon scattering tomography. The regular procedure to determine the scattering angle comprises the collection of exactly four hit locations in four detector layers among which two top detector layers are utilized to construct the first vector, whereas the second vector is built by using two bottom detector layers. Although this procedure acts to classify the target volumes in the tomographic systems based on the muon scattering, the scattering angle obtained through the usual methodology founded on four detector layers is dubious for not yielding any information about the position of the target volume. Nonetheless, the same set of four detector layers also imparts the possibility of splitting the scattering angle into two separate angles by creating a triangular correlation in such a way that the scattering angle is referred to an exterior angle, whereas the separate angles are considered the interior opposite angles that are not neighboring this exterior angle. In this study, we first show that a combination of three detector layers out of four fulfills the calculation of the interior opposite angles. Then, by employing the GEANT4 simulations over our tomographic configuration composed of three plastic scintillators in either section, we demonstrate that the interior opposite angles differ toward the vertical spatial variation, while the exterior angle approximately remains constant, thereby implying a beneficial feature to be used for the image reconstruction purposes.

Keywords: muon scattering tomography, scattering angle, exterior angle, interior angle, Monte Carlo simulations, GEANT4
DOI: 10.31526/JAIS.2022.247

1. INTRODUCTION

In the muon scattering tomography [1, 2, 3, 4], the scattering angle due to the volume of interest (VOI) and its associated statistics act as the principal variables in order to discriminate as well as to reconstruct the corresponding VOIs in the image reconstruction techniques such as Point-of-Closest Approach (POCA) [5, 6, 7, 8, 9, 10, 11]. As specified by the conventional tomographic configurations based on the muon scattering [12], the entire detection system regularly includes a bottom hodoscope below the VOI in addition to a top hodoscope above the VOI on the condition of multiple detector layers present at each hodoscope [6, 7, 10]. In these tomographic setups hinged on the muon scattering, the scattering angle is commonly computed by constructing a vector [13, 14, 15] founded on two hit locations at two distinct detector layers within every hodoscope. Although this prevalent procedure that is devoted to calculate the characteristic angular deviation anyway serves to differentiate the corresponding VOIs or to produce their radiographic images, the angular variation toward the spatial change of the same VOIs is not definitely assured by using the habitual definition of the scattering angle, which also means that the regular utilization of the two hit locations at each section might not yield any further information toward the position change of the target material.

In the present study, motivated by this question mark about the angular alteration by means of the common definition versus the spatial variation, we first show that the same set of four hit locations collected from the two detector layers at every hodoscope might lead to split the scattering angle into two opposite angles by forming a triangular correlation where the scattering angle is considered an exterior angle, while the two separate angles by definition are interior angles that are not neighboring the scattering angle. In the second place, we perform a series of GEANT4 simulations [16] by changing the vertical position of the VOI made out of stainless steel within our tomographic scheme [17] consisting of three plastic scintillators manufactured of polyvinyl toluene, and we demonstrate that the interior opposite angles vary depending on the VOI location, whereas the scattering angle that is expressed according to the regular definition does not yield a significant difference despite this spatial change. Last but not least, the triangular correlation between the scattering angle and the interior opposite angles is corroborated by the equality between the scattering angle and the sum of these nonadjacent angles via our GEANT simulations. The current study is organized as follows.

In Section 2, we define the scattering angle as well as the interior separate angles in accordance with the triangular correlation by delineating our tomographic configuration, and Section 3 is composed of our simulation schemes in order to explore the position sensitivity of the scattering angle as well as the opposite interior angles obtained by splitting the scattering angle. While we exhibit our simulation results in Section 4, we draw our conclusions in Section 5.

2. TRIANGULAR CORRELATION

To begin with, our tomographic setup is depicted in Figure 1(a) where the scattering angle indicated by θ is determined by building a vector at each section, the components of which are obtained through the hit locations on two detector layers. The scattering angle might be split into two opposite angles by setting up a triangular correlation as illustrated in Figure 1(b) where the exterior angle referred to as the scattering angle is equal to the superposition of the two non-adjacent angles.

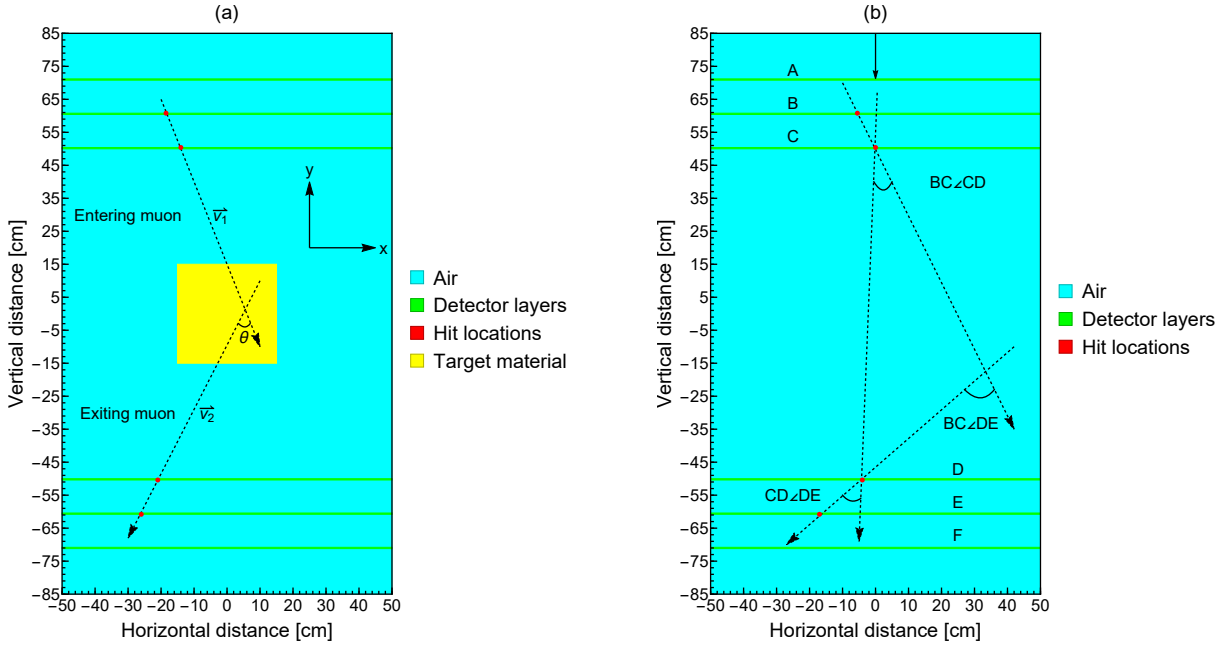


FIGURE 1: Delineation of angular deviation due to the target volume in our tomographic scheme: (a) scattering angle denoted by θ and (b) triangular correlation between $\theta = BC\angle DE$ and the interior angles denoted by $BC\angle CD$ and $CD\angle DE$ after splitting.

By reminding that the capital letters listed as A, B, C, D, E, and F in Figure 1(b) point to the hit locations in the specific detector layers, the conventional scattering angle denoted by θ that also refers to the exterior angle is commonly defined as written in [13, 14, 15]

$$\theta = BC\angle DE = BC\angle CD + CD\angle DE = \arccos\left(\frac{\vec{BC} \cdot \vec{DE}}{|\vec{BC}| |\vec{DE}|}\right). \quad (1)$$

The same set of four hit locations also gives access to compute two opposite interior angles as expressed in

$$BC\angle CD = \arccos\left(\frac{\vec{BC} \cdot \vec{CD}}{|\vec{BC}| |\vec{CD}|}\right), \quad (2)$$

$$CD\angle DE = \arccos\left(\frac{\vec{CD} \cdot \vec{DE}}{|\vec{CD}| |\vec{DE}|}\right). \quad (3)$$

It is worth mentioning that the computation of the interior angles indicated by $BC\angle CD$ and $CD\angle DE$ does not require any further data collection from the detector layers since the same set of four hit locations is already mandatory to calculate the scattering angle, and three hit points out of four are sufficient in order to determine these nonadjacent angles. The average angular deviation of any combination, i.e., $\overline{x\angle y}$, at a given energy value is determined by averaging over N number of the nonabsorbed/nondecayed muons as defined in

$$\overline{x\angle y} = \frac{1}{N} \sum_{i=1}^N (x\angle y)_i. \quad (4)$$

3. SIMULATION SCHEME FOR POSITION SENSITIVITY

Following the definition of the triangular correlation and the associated angles of this correlation collected based on the tracked hits from the detector layers, we perform a sequence of GEANT4 simulations in order to verify the triangular correlation as well as to testify for the position sensitivity. We define three position cases in cm that consist of origin, up, and down as delineated in Figures 2(a)–(c), where (a) shows the case called origin and the center of the VOI is located at (0, 0), (b) demonstrates the case labeled up and the center of VOI is moved to (30, 0), and (c) depicts the case termed down and the center of VOI is situated at (−30, 0). Apart from the VOI position, the VOI material is stainless steel with a cubic volume of $30 \times 30 \times 30 \text{ cm}^3$.

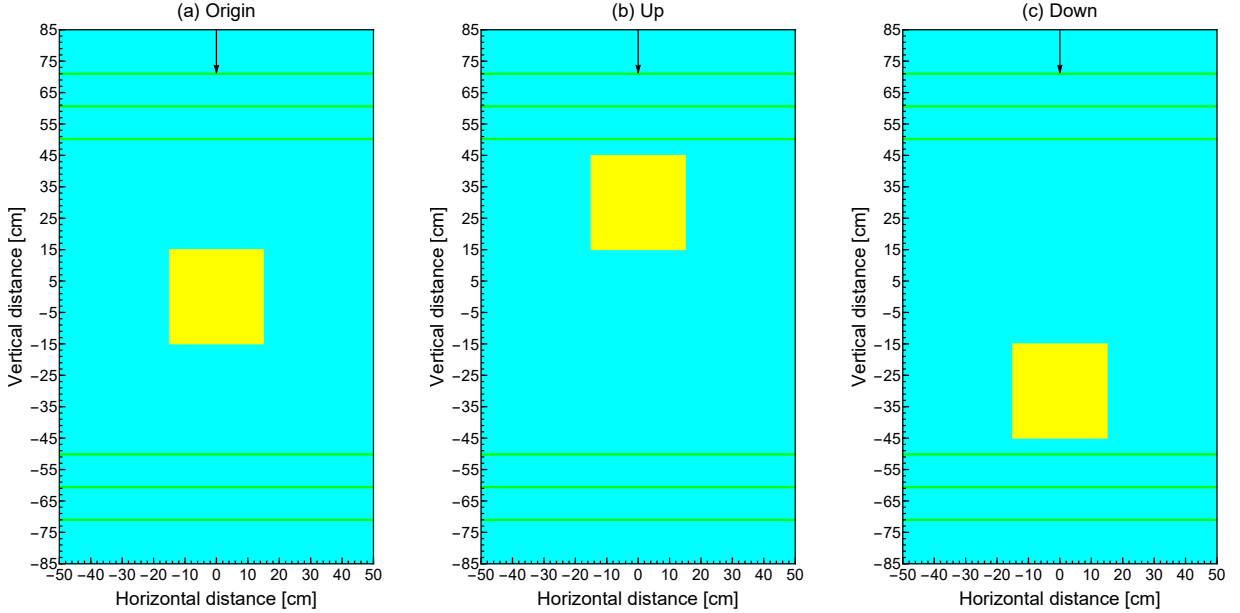


FIGURE 2: Simulation schemes for the position sensitivity by using three different vertical VOI centers with (a) origin at (0, 0), (b) up at (30, 0), and (c) down at (−30, 0) in cm.

To concisely summarize, our tomographic setup in GEANT4 simulations is composed of three plastic scintillators made out of polyvinyl toluene with the dimensions of $100 \times 0.4 \times 100 \text{ cm}^3$ at every section. We utilize a central monodirectional uniform muon beam as indicated by a downward black arrow in Figures 2(a)–(c), and the uniform energy distribution [18] lies on an interval between 0.1 and 8 GeV for the reason of more favorable numerical stability. Since the current aperture of the entire detection geometry commonly only accepts the narrow angles apart from the very rare entries around the corners, this beam setup is considered significantly reliable by reminding us that the distribution of the incident angle (α) approximately corresponds to $\cos^2(\alpha)$ for an interval between $-\pi/2$ and $\pi/2$ [19]. The number of the simulated muons in each defined position is 10^5 . The tomographic components in the GEANT4 simulations are defined in agreement with the G4/NIST database, and the preferred physics list is FTFP_BERT. The simulation features are listed in Table 1.

The muon tracking is accomplished by G4Step, and the tracked hit locations are postprocessed with the support of a Python script where the scattering angle and the interior nonadjacent angles are initially computed for every single nonabsorbed/non-decayed muon, then the uniform energy spectrum limited by 0.1 and 8 GeV is divided into 16 bins by marching with a step of 0.5 GeV, and each obtained energy bin is labeled with the central point in the energy subinterval. Finally, the determined angles are averaged for the associated energy bins.

4. SIMULATION OUTCOMES

We commence our simulations with the scattering angle denoted by BC/DE in order to investigate its position sensitivity versus the vertical displacement, and Figure 3(a) shows the average BC/DE as a function of the kinetic energy. We observe that the average BC/DE does not exhibit a tendency to vary with the vertical position change as demonstrated in Figure 3(a).

Whereas the average BC/DE remains almost constant in spite of the spatial variation, the average interior nonadjacent angles indicated by BC/CD and CD/DE yield three distinct curves in the three different vertical positions as shown in Figures 3(b) and (c). Another reflection that we notice from Figures 3(b) and (c) is the opposite numerical trend among the opposite interior angles, which means that the average BC/CD increases in terms of the vertical boost, while CD/DE augments by the downward drop. At long last, we verify the triangular correlation as defined in equation (1), and Figure 3(d) ratifies the equality between the scattering angle and the superposition of the interior nonadjacent angles through our GEANT4 simulations over three different positions.

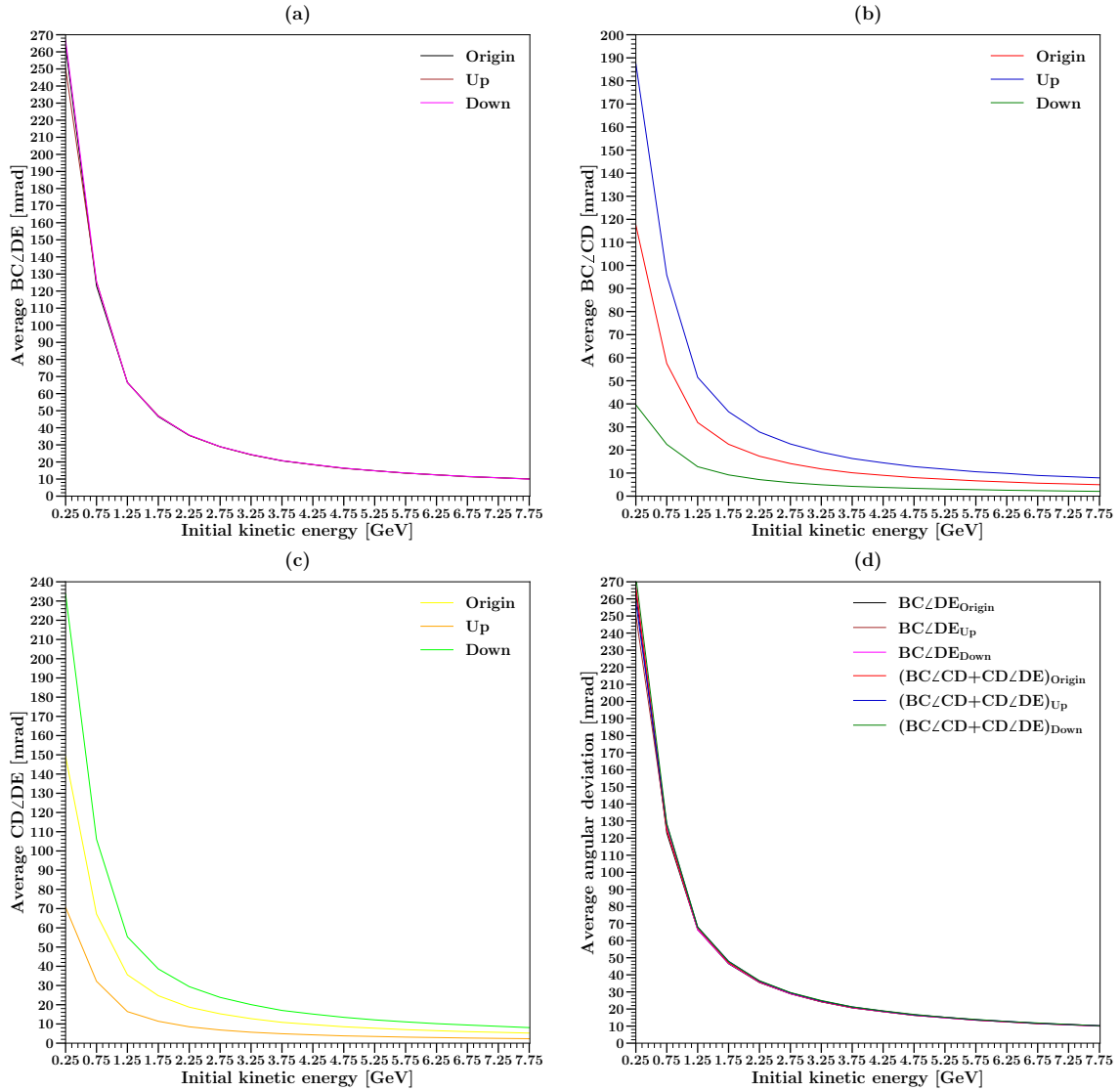


FIGURE 3: Comparison between the average angular deviations over (a) BC/DE, (b) BC/CD, (c) CD/DE, and (d) sum of BC/CD and CD/DE for three different positions.

5. CONCLUSION

In this study, we explore the triangular correlation of angular deviation by means of our GEANT4 simulations. Upon our simulation outcomes, we explicitly observe that the conventional scattering angle remains constant toward the position change of the target material, whereas the opposite interior angles exhibit differences due to this spatial variation, therewith hinting a beneficial property to be utilized for the image reconstruction purposes.

APPENDIX: AN EXAMPLE OVER BC/DE

The scattering angle calculation for BC/DE is performed by using the following Python statements:

```
import sys
import math
import statistics

def calculateAngle(x,y,z):\
    tetaP1 = (x[0]*x[1]) + (y[0]*y[1]) + (z[0]*z[1])\
    tetaP2 = math.sqrt((x[0]**2)+(y[0]**2)+(z[0]**2))*math.sqrt((x[1]**2)+(y[1]**2)+(z[1]**2))\
    teta = math.acos(tetaP1 / tetaP2)\
    teta = teta * 1000\
```

TABLE 1: Simulation features.

Particle	μ^-
Beam direction	Vertical
Momentum direction	(0, -1, 0)
Source geometry	Planar
Initial position (cm)	([-0.5, 0.5], 85, [-0.5, 0.5])
Number of particles	10^5
Energy distribution	Uniform
Energy interval (GeV)	[0, 8]
Bin step length (GeV)	0.5
Energy cut-off (GeV)	0.1
Target material	Stainless steel
Target geometry	Cube
Target size (cm)	30
Material database	G4/NIST
Reference physics list	FTFP_BERT

```

return teta\\

try:
    data_input = open(" position_sensitivity.csv", "r")
except:
    raise Exception("File doesn't exist!")

try:
    data_output= open("angle.txt", "w")
except:
    data_input.close()
    raise Exception("Can't create output file!")

data_list = data_input.readlines()
data_list.pop(0)

event_num=-1
kinetic_energy=0.0
vector_counter=0
angle_value=0.0
x_value=0.0
y_value=0.0
z_value=0.0
x_vector=[0.0,0.0]
y_vector=[0.0,0.0]
z_vector=[0.0,0.0]
max_energy=0.0
last_kinetic_energy = 1.0
nonzero_kinetic_energy = True

for x in data_list:
    line_list=x.split(",")
    if line_list[0] != event_num:
        #initial line
        if event_num == -1:
            event_num = line_list[0]
            kinetic_energy = float(line_list[4])/1000
            vector_counter = 1
            x_value=float(line_list[1])
            y_value=float(line_list[2])
            z_value=float(line_list[3])
            switch = True
        #different event
        else :
            if(last_kinetic_energy > 0.0):
                nonzero_kinetic_energy = True

```

```

else:
    nonzero_kinetic_energy = False
if switch :
    if vector_counter == 4:
        if nonzero_kinetic_energy:
            data_output.write(event_num + " " + str(kinetic_energy)
                               + " " + str(angle_value) + "\n")
        if kinetic_energy > max_energy:
            max_energy = kinetic_energy
event_num = line_list[0]
kinetic_energy = float(line_list[4])/1000
x_value=float(line_list[1])
y_value=float(line_list[2])
z_value=float(line_list[3])
x_vector=[0.0,0.0]
y_vector=[0.0,0.0]
z_vector=[0.0,0.0]
vector_counter = 1
angle_value = 0.0
switch = True
#same event
else :
    last_kinetic_energy = float(line_list[4])/1000
    vector_counter += 1
    if vector_counter == 2:
        x_vector[0] = float(line_list[1]) - x_value
        y_vector[0] = float(line_list[2]) - y_value
        z_vector[0] = float(line_list[3]) - z_value
        x_value=float(line_list[1])
        y_value=float(line_list[2])
        z_value=float(line_list[3])

    if vector_counter >= 3:
        x_vector[1] = float(line_list[1]) - x_value
        y_vector[1] = float(line_list[2]) - y_value
        z_vector[1] = float(line_list[3]) - z_value
        x_value=float(line_list[1])
        y_value=float(line_list[2])
        z_value=float(line_list[3])
        try:
            angle_value = calculateAngle(x_vector,y_vector,z_vector)
            switch = True
        except ZeroDivisionError:
            switch = False
        except:
            print("zomg exception occured!")
            switch = False

#final line
if switch:
    if vector_counter == 4:
        if (last_kinetic_energy > 0.0):
            data_output.write(event_num + " " + str(kinetic_energy) + " " + str(angle_value))
        if kinetic_energy > max_energy:
            max_energy = kinetic_energy

#####Part 2 - Average
data_input.close()
data_output.close()

#Calculate average and std-dev
try:
    data_input = open("angle.txt", "r")
except:
    raise Exception("File doesn't exist!")

try:
    data_output= open("angle-average.txt", "w")

```

```

except:
    data_input.close()
    raise Exception("Can't create output file!")

input_list = data_input.readlines()
line_list.clear()
bin_list = []
for x in range(2*(int(max_energy)+2)):
    bin_list.append([])

#seperate into bins
for x in input_list:
    line_list=x.split(" ")
    energy_value = float(line_list[1])
    bin_value = 0.5 if math.modf(energy_value)[0] < 0.5 else 1
    bin_value += math.modf(energy_value)[1]
    bin_index = int(bin_value * 2)
    output_value = float(line_list[2])
    bin_list[bin_index].append(output_value)

#print output in new format
for x in range(len(bin_list)):
    if not bin_list[x]:
        continue
    gev_num = float(0.5/2+(x-1)*0.5)
    occurance = len(bin_list[x])
    average_output = statistics.mean(bin_list[x])
    if occurance > 1:
        std_dev_output = statistics.stdev(bin_list[x])
    else:
        std_dev_output = 0
    max_gev = 8.5
    min_gev = 0.0
    if gev_num > min_gev :
        if gev_num < max_gev:
            data_output.write(str(gev_num) + " " + str(occurance) + " " + str(average_output)
                + " " + str(std_dev_output) + "\n")

data_input.close()
data_output.close()

```

CONFLICTS OF INTEREST

The authors declare that there are no conflicts of interest regarding the publication of this paper.

References

- [1] Silvia Pesente et al. First results on material identification and imaging with a large-volume muon tomography prototype. *Nucl. Instr. Meth. A*, 604(3):738, 2009.
- [2] P. Checchia. Review of possible applications of cosmic muon tomography. *J. Instrum.*, 11(12):C12072, 2016.
- [3] S. Procureur. Muon imaging: Principles, technologies and applications. *Nucl. Instr. Meth. A*, 878:169, 2018.
- [4] Lorenzo Bonechi et al. Atmospheric muons as an imaging tool. *Rev. Phys.*, 5:100038, 2020.
- [5] Larry Joe Schultz. *Cosmic ray muon radiography*. PhD thesis, Portland State University, 2003.
- [6] Marilena Bandieramonte et al. Automated object recognition and visualization techniques for muon tomography data analysis. In *2013 IEEE Int. Symp. Technol. Homel. Secur. (HST)*, page 517, 2013.
- [7] Baihui Yu et al. Preliminary analysis of imaging performance in cosmic-ray muon radiography. In *2013 IEEE Nucl. Sci. Symp. Med. Imaging Conf. (NSS/MIC)*, page 1, 2013.
- [8] Zhengzhi Liu et al. Muon tracing and image reconstruction algorithms for cosmic ray muon computed tomography. *IEEE Trans. Image Process*, 28(1):426, 2018.
- [9] Guangliang Yang et al. Novel muon imaging techniques. *Philos. Trans. R. Soc. A*, 377(2137):20180062, 2019.
- [10] Weihe Zeng et al. Principle study of image reconstruction algorithms in muon tomography. *J. Instrum.*, 15(02):T02005, 2020.
- [11] Zhengzhi Liu et al. Muon-computed tomography using POCA trajectory for imaging spent nuclear fuel in dry storage casks. *Nucl. Sci. Eng.*, 2021.
- [12] Konstantin Borozdin et al. Radiographic imaging with cosmic-ray muons. *Nature*, 422(6929):277, 2003.
- [13] T. Carlisle et al. Multiple Scattering Measurements in the MICE Experiment. Technical Report FERMILAB-CONF-12-171-APC, Fermi National Accelerator Lab. (FNAL), 2012.
- [14] John Columba Nugent. *Multiple Coulomb scattering in the MICE experiment*. PhD thesis, University of Glasgow, 2017.

- [15] Dan Poulson et al. Application of muon tomography to fuel cask monitoring. *Philos. Trans. R. Soc. A*, 377(2137):20180052, 2019.
- [16] Sea Agostinelli et al. GEANT4 - a simulation toolkit. *Nucl. Instr. Meth. A*, 506(3):250, 2003.
- [17] Anzori Georgadze et al. Method and apparatus for detection and/or identification of materials and of articles using charged particles, 2021. US Patent App. 16/977,293.
- [18] V. Anghel et al. A plastic scintillator-based muon tomography system with an integrated muon spectrometer. *Nucl. Instr. Meth. A*, 798:12, 2015.
- [19] Bryan Olmos Yáñez and Alexis A Aguilar-Arevalo. A method to measure the integral vertical intensity and angular distribution of atmospheric muons with a stationary plastic scintillator bar detector. *Nucl. Instr. Meth. A*, 987:164870, 2021.